energies

MDPI

Article

Analysis of a Parallel Hybrid Electric Tractor for Agricultural Applications

Francesco Mocera * and Aurelio Somà

Department of Mechanical and Aerospace Engineering, Politecnico di Torino, Corso duca degli Abruzzi 24, 10129 Torino, Italy; aurelio.soma@polito.it

* Correspondence: francesco.mocera@polito.it

Received: 2 May 2020; Accepted: 1 June 2020; Published: 12 June 2020

Abstract: The field of Non-Road Mobile Machineries (NRMM) is now more than ever considering the adoption of electric systems to reduce the amount of pollutant emissions per unit of work. However, the intensity and complexity of the tasks performed by a working machine during its life is an obstacle to the widespread adoption of electric systems. Specific design solutions are required to properly split the power output of the hybrid powertrain among the different loads (wheel, power take off, hydraulic tools, etc.). In this work, a performance analysis between a traditional agricultural tractor and a proposed hybrid electric architecture of the same vehicle is shown. The comparison was performed on a set of tasks characterized on a real orchard tractor which were used to build the input signals of two different numerical models: one for the traditional diesel architecture and the other for the hybrid electric solution. The two models were tested with the same operating tasks to have a one to one comparison of the two architectures. Peak power capabilities of the hybrid solution and performance of the Load Observer energy management strategy were investigated to validate the feasibility of the proposed solution.

Keywords: hybrid electric tractor; non-road mobile machineries; hybrid electric vehicles; energy management; numerical simulation

1. Introduction

The electrification process that is involving all the transportation field is a trend deriving from the need for a lower impact on air quality, especially in the production of CO_2, NO_x, and particulate matter [1–4]. However, transportation is not the only contributor to air pollution [5,6]. Industrial processes, agriculture, and residential and commercial buildings also play a big role in the production of the aforementioned pollutants as well as for other unhealthy substances. Industrial heavy-duty vehicles, especially in agriculture, construction, and handling, combine the type of pollutant production of transports, due to the use of the same propulsion units, with the massive quantities usually related to industrial processes and their power demanding tasks. For this reason, in the last decade, strict regulations were progressively applied to the Non-Road Mobile Machineries (NRMMs) [7–11] to push manufacturers towards the design of machines with the lowest possible environmental impact. Traditionally, NRMM have been equipped with high power diesel engines known for their robustness and reliability when subjected to heavy duty tasks in harsh environments. Nowadays, this propulsion system is a mature technology both from the performance and manufacturing point of view which translates in a very attractive value of the ratio between performance (power output) and Total Cost of Ownership (TCO). However, the environmental impact of this type of propulsion system is well known in the scientific community [12–15]. To meet national and international regulations on pollutant emissions that would prevent sales of non-compliant NRMMs exceeding pollutants emissions, the use of exhaust gas after-treatment systems has been the most widely accepted method

among manufacturers. However, the most recent regulations will require very complex, cumbersome, and expensive exhaust after-treatment systems to properly filter the pollutants out from the gas stream at the pipeline [16–18]. Filtering systems can be very space consuming on industrial vehicles. To be competitive, the available on-board space on industrial vehicles should be used to implement new productivity features and functionalities rather than just allowing the machine to operate in compliance with regulations. This is one of the reasons why several NRMM manufacturers and researchers started to explore hybrid electric systems as alternative propulsion units [19–23]. The optimal hybridization level of the architecture [24,25] allows increasing the overall efficiency of the machine reducing the amount of pollutants produced per unit of work [26]. Moreover, hybrid and electric solutions allow introducing new functionalities for a given on board volume thanks to the high level of flexibility of electric and electronic drives. The possibility to work in full electric mode allows using the same machine in closed environments and low emissions zones in the city centre, opening a machine to completely new market scenarios.

Recently, both manufacturers and the scientific community have shown an increasing interest towards electric powertrains for agricultural tractor. In [27], Moreda et al. reviewed the actual state of the art in tractor electrification research, highlighting the characteristics of an electric or hybrid tractor architecture. A tractor powertrain must be able to provide power to different users: the driveline to propel the vehicle; the Power Take Off (PTO) if power needs to be transferred to one or more external units (usually called implements); the hydraulic system for machines that use hydraulic tools and actuators to perform heavy tasks (handling, lifting, processing, etc.). This power split can be achieved electrically in a series configuration as in [28] or mechanically with proper gearboxes or parallel configurations [29]. A proper energy management strategy becomes a crucial point if several paths need a comparable amount of power to perform a certain task. To the authors' knowledge, very few studies explored numerically performance of agricultural electric tractors and their control strategies [30–33]. However, now more than ever, practical use cases can be found in the literature [29,32,34]. In this work, a critical performance comparison between a traditional orchard tractor and the proposed hybrid solution was performed. Nowadays, orchard tractors represent a very specialized tractor family where the availability of on-board space is limited, so the energy storage system and the energy management strategy should be carefully designed to fulfill the most common working cycles of the machine. Thus, the design of the battery pack for this particular application is critical. Not only could a poorly design pack strongly affect the current peculiar characteristics of these vehicles but it could also strongly affect the costs of the final vehicle, affecting the overall success of the solution. The battery pack represents a critical part of every batteries based electric vehicles. This is particularly true for NRMM and their specific loading profiles. New design and testing methodologies have already been proposed in the literature addressing the use of LiB in heavy duty working vehicles [35–37].

In this study, a parallel hybrid architecture for an orchard tractor was investigated according to a set of field working scenarios to investigate the effectiveness of the adoption of this technology in such a particular field of application. The tasks were derived from an experimental activity described in Section 2 aimed to characterize performance of a traditional diesel-powered orchard tractor during its most common daily activities. Measurements were used to size the components of the two different numerical models presented in Section 3: one for the traditional diesel powered vehicle and the other for the proposed hybrid architecture. Models were compared in terms of peak power performance to study the proposed solution and its energy management strategy during similar loading scenario, as described in Section 4.

2. Experimental Analysis of Tractor Performance

Because of the wide variety of NRMM and the lack of standardized testing procedures, any analysis focused on NRMM performance comparison should start from the field, looking at their most common use cases. The proper combination of elementary tasks can result in representative

working cycles to be use in performance analysis. In this work, the analysis started from measurements of field performance of an orchard tractor during some of the most common tasks that these vehicles can approach. The characteristics of the orchard tractor considered for this work are shown in Table 1.

Table 1. Main characteristics of the orchard tractor.

Vehicle Properties	
Mass	2500 kg
Nominal power	75 kW @ 2300 rpm
Vehicle wheelbase	1900 mm
Max vehicle width	1850 mm
Number of possible gear ratios	36
Top speed	40 km/h
Minimum speed	0.4 km/h

To characterize the tractor daily activities, the attention focused on the monitoring of engine data and of driver commands available on the CAN BUS network of the vehicle [38] according to the SAE J1939 standard [39], very common in heavy duty applications. The attention mainly focused on the following parameters:

- The driver pedal signal as reference of the desired the working speed
- The engine rotational speed
- The actual engine load estimated by the VCU according to the characteristic map of the engine
- Vehicle speed

Data were collected from the CAN BUS network using a USB CAN Analyzer connected to a personal computer installed on the vehicle. The acquisition system was in a pure listening mode to prevent any undesired influence on the CAN BUS communication of the machine. The raw CAN BUS data was then post-processed to obtain the parameters of interest in a useful numeric format. The experimental activity focused on the monitoring during some specific tasks chosen as representative of the most common activities performed by an orchard tractor. The authors here identified one possible use case scenario for the vehicle which does not aim to represent all the possible tasks combination but can represent a realistic use of the machine. Data were collected during the following working operations:

- Transportation with empty and fully loaded trailer
- Use of a shredding implement
- Use of a rotary harrow implement
- Use of an atomizer implement

In Figure 1, data collected during the acceleration test with a fully loaded trailer (6000 kg mass) are shown to give a picture of the type of information available. This test consisted in a complete acceleration from 0 km/h to the maximum speed (around 40 km/h). Despite the overall high mass to be moved (tractor, trailer, and goods), the capabilities of engine exceeded the average power required by the application as demonstrated by the engine load at top speed. This is a typical example of a task where the installed engine is clearly oversized in terms of power required to perform it. In Table 2, a general overview on the characteristics measured during each of the activities mentioned before are shown in terms of average or Min/Max value registered. The experimental activity highlighted the multi-purpose nature of the machine. Depending on the main use of the tractor made by the farmer, the typical power demand can change significantly, at least in terms of peak capabilities. This justifies the need for oversized diesel engines that could at least approach all the possible working scenarios. However, measurements showed that the average power demand is quite lower with respect to the engine capabilities which could justify the adoption of a hybrid electric architecture with a downsized

diesel engine. In this case, the thermal unit could be sized to cover the average load leaving the peaks to the most efficient electric system.

Table 2. Tasks experimental characterization overview: (a) Trailer 6000 kg; (b) Trailer 1400 kg; (c) Atomizer; (d) Shredder; and (e) Rotary harrow.

	a	b	c	d	e
Work time (h)	0.017	0.05	0.065	0.18	0.2
Speed (km/h)	30/40	30/40	3.4	5	3.4
PTO speed	-	-	540	540	540
Engine Load (%)	50/100	40/100	70/75	45/60	65/90
Fuel (L)	0.1	0.3	0.9	1.1	2.5

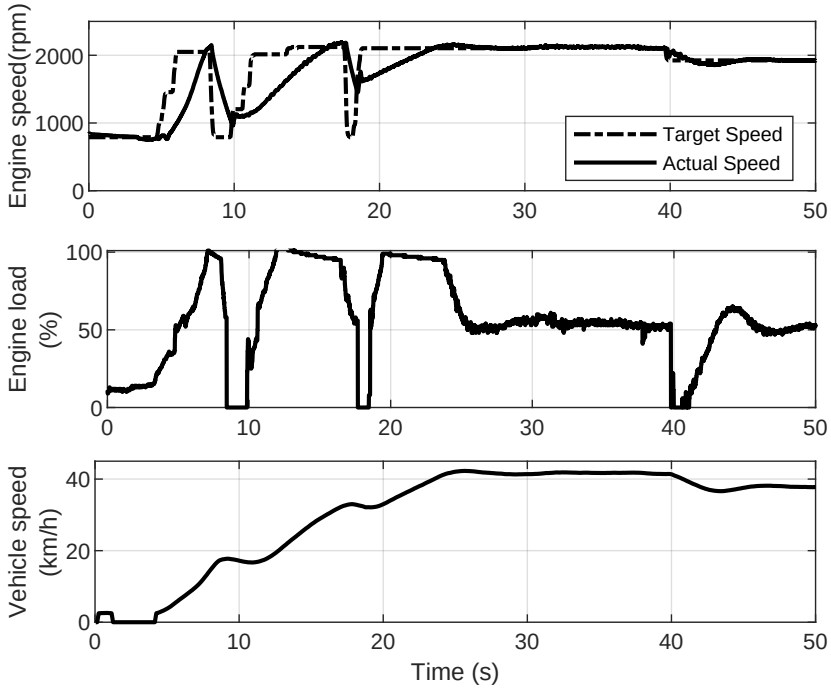

Figure 1. Acceleration test—fully loaded trailer 6000 kg.

3. Numerical Methods

The use of numerical simulations is crucial when it comes to the design of new hybrid electric powertrain topologies, as shown by several authors in the literature [24,25,35]. In this work, two numerical models were designed to perform a comparative analysis: one representing the traditional diesel powered architecture of an orchard tractor for agricultural applications and the other consisting of the same vehicle characteristics but powered by a parallel hybrid electric powertrain. The main goal of the first model was to replicate the actual tractor on the virtual environment. The use of experimental data allowed characterizing the main mechanical properties of the traditional tractor model as well as of the trailer used in some of the case studies. Then, the model was modified in terms of the propulsion subsystem. A parallel hybrid electric powertrain with a downsized diesel engine was proposed and included in the model maintaining the overall mechanical architecture. This allowed for a direct performance comparison between the two architectures for given working tasks.

3.1. Traditional Tractor Model

Modeling an agricultural tractor is quite a demanding task due to complexity of the mechanical architecture and of the power split among its several subsystems. Modern agricultural tractors are machines designed to accomplish several heavy tasks as:

- Pulling trailers on the road or ploughs in the fields
- Lifting objects using front or rear mounted hydraulic loaders
- Pushing terrain or snow with buckets or snowplough equipment
- Transfer power to external devices, usually called implements, designed to accomplish specific working tasks but without any autonomous propulsion unit

A representative numerical model of an agricultural tractor must be able to describe subsystems from several physical domains. As shown in Figure 2, a Physical Network (PN) [40] modeling approach was chosen to model the architecture of both the traditional and hybrid electric power unit of the tractor considered for this study. The PN is a modular modeling approach where each element is considered as a physical entity capable of exchanging energy with all the other subsystems to which it is connected. Each element is characterized by two types of variables: Across and Through variables. In each physical domain, the product of an Across and Through variable gives the power exchanged by a certain physical element with all the others to which it is connected. Thus, the solution of the systems must satisfy the power balance equations for each component at each time step.

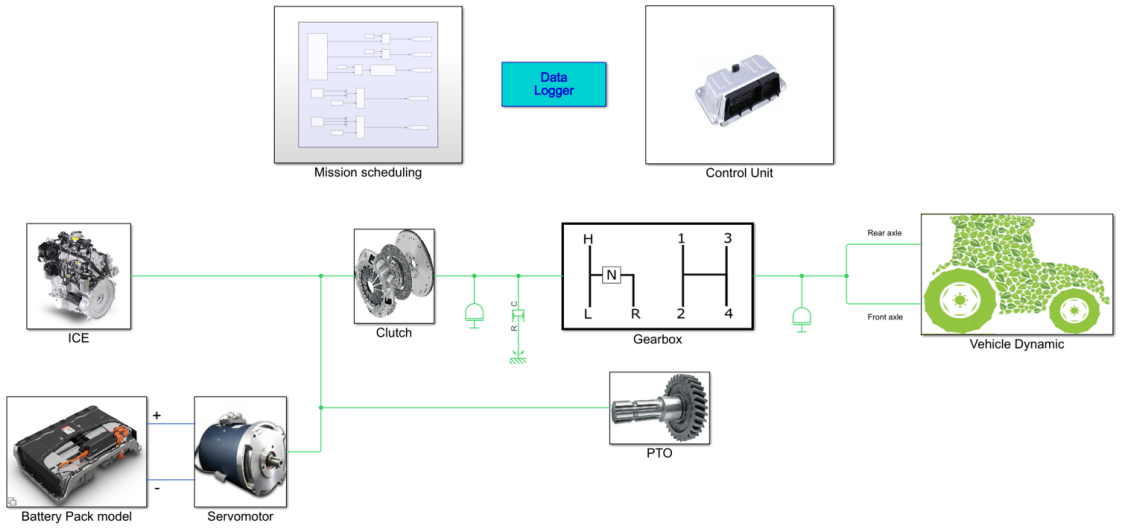

Figure 2. Tractor architecture model.

The following aspects were covered when modeling the traditional tractor architecture:

- Vehicle and trailer (if present) dynamics
- Gearbox and clutch
- Engine
- Vehicle Control Unit (VCU)
- PTO loads

The tractor dynamic was described using a 1D longitudinal dynamic model shown in Figure 3 and given by the following equations:

$$m\dot{V}_x = 2\left(F_{xf} + F_{xr}\right) - F_d - mg \cdot sin\beta \quad (1)$$

$$F_{zf} = \frac{-h\,(F_d + mg \cdot sin\beta) + b \cdot mg \cdot cos\beta}{2(a+b)} \tag{2}$$

$$F_{zr} = \frac{+h\,(F_d + mg \cdot sin\beta) + a \cdot mg \cdot cos\beta}{2(a+b)} \tag{3}$$

where:

- a, b, and h represent the relative position of the centre of gravity of the vehicle with respect to the front and rear axles.
- m is the tractor mass, g the acceleration of gravity.
- β is the road slope angle.
- V_x is the vehicle longitudinal speed.
- F_d is the aerodynamic drag force as $F_d = 0.5\rho C_d A {V_x}^2 \cdot sign(V_x)$, with ρ the air density, C_d the drag coefficient, and A the frontal cross sectional area of the vehicle.
- F_{xf} and F_{xr} are the contact forces between the wheels and the ground on the longitudinal direction (front and rear axle).
- F_{zf} and F_{zr} are the normal contact forces between the wheels and the ground (front and rear axle).

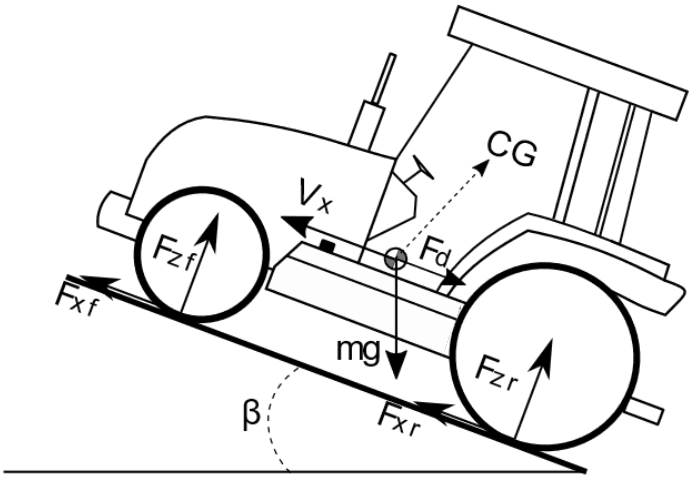

Figure 3. 1D Longitudinal model of the tractor.

The trailer was modeled with the same approach, considering that the driving force does not come from the driven wheels but from the so called three points hitch system. From the dynamic point of view, if the connection between the tractor and the trailer is considered rigid, they will share the same longitudinal speed. The vehicle model was powered by the energy coming from the engine through the gearbox. Agricultural tractors gearboxes are well known for the high number of gear ratios they can provide. This allows the driver to have the full power of the engine at different operating vehicle speeds according to the specific working task to be performed (plough, harrowing, transportation, etc.). To replicate this flexibility, the gearbox was modeled as follows:

- A first pair of gears to have an overall speed reduction of about 75% between the input and the output shaft of the gearbox
- Two pairs of gears for two different working ranges: Low speed and High speed
- Four pairs of gears to realize four different gear ratios within each speed range

Each pair of gears was engaged during simulation through a logic signal actuation command according to the records of the gears engaged by the real driver during the tests. The main clutch of the driveline was modeled using a traditional Coulomb friction model [41]. The engagement starts according to a signal that linearly increases the normal contact force between the two elements

connected, respectively, to the input and output shaft. In this model, after a certain slip governed by the dynamic friction coefficient, the clutch is considered fully engaged when the two shaft rotates at the same rotational speed. At this point, the maximum torque transmittable is determined by the static friction coefficient. Modeling the clutch was a crucial step in order to be able to shift gears during the simulations.

Another element of the numerical model was the engine block. This subsystem had to simulate two aspects of a traditional engine: the power output as a combination of torque and speed and the instantaneous fuel consumption according to the current operating point of the engine. Engine power was modeled as described in [40] with a normalized polynomial function:

$$p(w) = 0.6526w + 1.6948w^2 - 1.3474w^3 \tag{4}$$

where $w = \frac{\Omega}{\Omega_0}$ is the engine speed Ω normalized with respect to the engine speed at which the engine provides the maximum power P_{max}. It is clear that, given the characteristic of the engine in terms of operating speed $[\Omega_{min}, \Omega_{max}]$, maximum power P_{max}, and its related rotational speed Ω_0, the power output of the engine is known for each given rotational speed. Thus, the instantaneous torque T can be obtained as

$$T = \frac{P_{max}}{\Omega_0} \frac{p(w)}{w} \tag{5}$$

The parameters for this model of the engine were defined for each of the two engines used in the two architectures. Another important aspect covered by the engine model was the estimation of the fuel consumption during operating conditions. In this case, a model proposed by the Nebraska Test Laboratory [42] was used. This model is the result of a statistical analysis on fuel consumption on a large set of agricultural tractors during field operations. According to the formulation proposed by the authors, the fuel consumption was evaluated as

$$Q_F = (0.0434 \cdot X + 0.019) \cdot P_{nom} \tag{6}$$

$$Q_R = Q_F \cdot [1 - (N - 1) \cdot (0.45 \cdot X + 0.877)] \tag{7}$$

where:

- Q_F is the diesel fuel consumption at partial load and full throttle (gal/h).
- Q_R is the diesel fuel consumption at partial load and reduced throttle (gal/h).
- X is the actual engine load expressed as the ratio of the actual engine output power over the maximum power available at the same speed (decimal).
- P_{nom} is the nominal engine power (hp).
- N is the ratio between the actual engine speed and the nominal speed at which P_{nom} is evaluated.

The main reason behind the choice of this model relied on the parameters considered for the fuel consumption estimation. It is reasonable to correlate the fuel consumption to the size of the engine (given by P_{nom}), the actual engine load, and its working speed. This parametric model allowed useful relative comparison with the diesel engine considered for the proposed hybrid architecture. The engine was controlled in the simulation environment with an engine speed controller to replicate the real control architecture of the most common tractors available on the market. The parameters of the PI (Proportional-Integral) controller designed for this model were set to best fit the engine speed measured during the tests.

Finally, the modeling of the PTO loads applied by each implement attached to the tractor was approached. Due to the lack of information about the internal design of each implement considered during the tests, an inverse approach was used. First, the validation of the vehicle model with the standard diesel engine unit was performed. Then, knowing the amount of power required for a certain working speed (given by the vehicle model), the numerical PTO load was controlled on the traditional

tractor model to apply the right torque to have the same engine load measured during the same activity. Figure 4 shows the work-flow followed to estimate the PTO loads given the experimental measurements and the numerical vehicle model of the tractor. A PI controller was used to make sure that, during those simulations where the tractor was used to pull and provide power to the external implement, the simulated engine load was as close as possible to the measured one. The authors are aware of the approximation made with this assumption. However, the type of analysis the models were designed for did not require a highly detailed model on the power used by the external implement but about the load applied to the engine. This information was the key point in the comparison between the traditional and the proposed architecture.

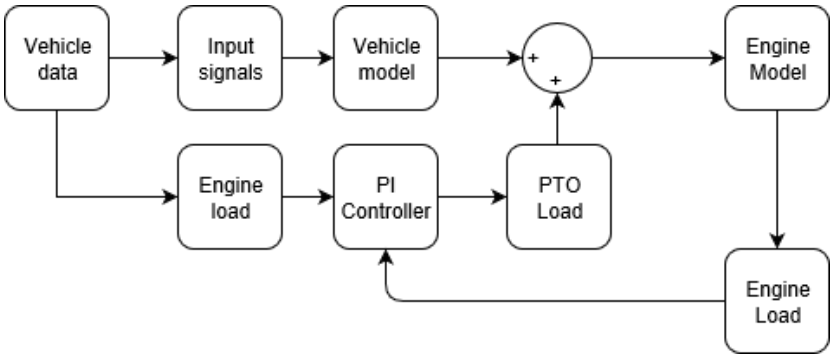

Figure 4. PTO load modeling approach.

3.2. Hybrid Electric Tractor Model

The hybrid electric architecture considered for this analysis was a parallel hybrid system with a downsized diesel engine [21,24]. Two reasons motivated the use of a smaller engine:

- Most of the time orchard tractors are equipped with oversized engines to cover all the possible peaks in power demand the machine could face during its entire life. However, bigger engines have higher fuel consumption because of their construction, thus they become less efficient if the nominal power is used few times during the whole life of the vehicle.
- Modern regulations on pollutant emissions are divided into power classes. Thus, using a smaller engine, it is possible to stay in a low power application class where the restrictions on the amount of pollutants require the use of fewer additional after-treatment components.

The use of an electric unit in parallel to the smaller thermal engine allowed maintaining the same performance level in terms of peak power capabilities. To implement the electric system in the tractor model as shown in Figure 2, the following aspects were covered:

- Implementation of an electric unit (electric motor and simplified electronic drive) to add power to the driveline path
- Implementation of a LiB ESS to provide electric power to the drive and the motor
- Design of a control algorithm to split the power demand between the thermal and electric unit

From the modeling point of view, the use of the PN allowed including the electric system within the same environment stated that the power balance equations must be verified at each integration step among all the subsystem. The proposed electric motor had the characteristics shown in Table 3. These characteristics were combined to those of the new thermal unit, characterized by a nominal power of 54 kW at 2300 rpm. Thus, the overall combined power output of the hybrid unit can be higher than the maximum power of the traditional architecture (72 kW @ 2300 rpm).

Table 3. Electric motor characteristics.

Motor Properties	
Nominal speed	2300 (rpm)
Nominal power	30 kW
Maximum torque	130 Nm
Nominal efficiency	95%

The electric power for the hybrid system was provided by a battery pack model consisting of a series connection of the cell studied by the authors in previous works available in the literature [35–37]. Briefly, each single cell was modeled as a single Equivalent Circuit Model (ECM), the behavior of which depends on a set of parameters variable with the actual State of Charge (SoC) of the cell. Once the parameters are stated, an ECM provides the instantaneous cell voltage for a given discharging/charging current. Thus, the instantaneous electric power (voltage times current) provided by the ESS was equal to the power required by the servo motor according to the PN approach.

Finally, the energy management strategy to coordinate the electric and thermal unit according to the driver needs was defined. As described in Figure 5, the control strategy had a master–slave control configuration denominated by the authors' Load Observer. The main goal of this algorithm was to use as much as possible the thermal unit as the primary (master) energy source. Actually, this is crucial if the overall goal is to minimize the size of the ESS: the more the system relies on the thermal engine, the lower is the amount of electric energy to be stored on board to accomplish the daily activities. The electric system was the slave element in this control layout. Its main role was to help the diesel engine in case of peaks in the power demand. To do that, the control strategy was based on the continuous monitoring of the actual engine load. The engine load is the ratio between maximum power of the engine for a given rotational speed and the actual power output. This index was the key parameter of the Load Observer strategy. The electric system is controlled to provide the necessary torque to maintain the reference speed set by the driver. An increase of the external load would require extra power to maintain the same reference speed. However, the control signal for the electric system was always weighted by a function of the actual engine load. In this way, it was possible to increase the amount of power requested to the engine having a consistent electric motor boost only above a certain level of power demand. The interesting point of this strategy was that, depending on the type of weighting function and used parameters, it was possible to change the overall behavior of the machine depending on the heaviness of the tasks. The flexibility of the electric drive would add this capability to the tractor to optimize the power output according to the driver needs.

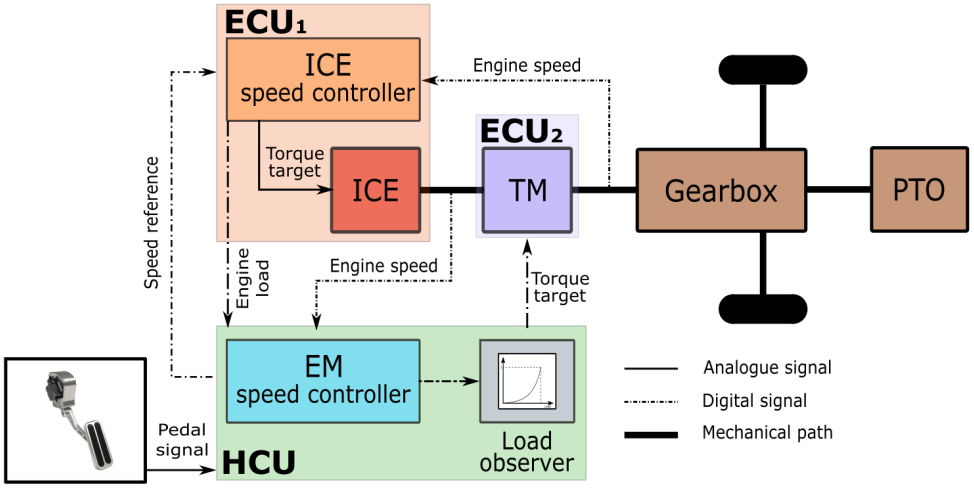

Figure 5. Master–slave control strategy with engine Load observer.

4. Results and Discussion

In this section, the main numerical results of this work are shown. First, a comparison between the model of the diesel architecture and the experimental results is addressed. The comparison allowed validating the dynamic behavior of the numerical vehicle model as well as the process to simulate the PTO loads. The mechanical structure of the simulated tractor was then used for the simulation of the hybrid electric architecture. Given the same tasks, performance of the two systems were compared in terms of power capabilities to understand if the electric system was able to satisfy power demand. The analysis allowed testing also the Load Observer energy management strategy in terms of power split among the two power units and of operational stability.

4.1. Tractor Model Validation

To validate the tractor model, a comparison between experimental measurements and the simulation of the same tasks was performed. The vehicle model was compared using an acceleration test performed with a trailer at full load. The driver pedal signal was assigned as input of the model together with a properly reconstructed signal to represent the gear shifts. The pedal signal represented the desired working speed for the speed-controlled diesel engine. As shown in Figure 6, the simulated acceleration test well represents the test performed, especially in terms of vehicle speed. This comparison allowed validating the gearbox model as well as the wheel model, especially in terms of rolling radius which affects the overall vehicle speed.

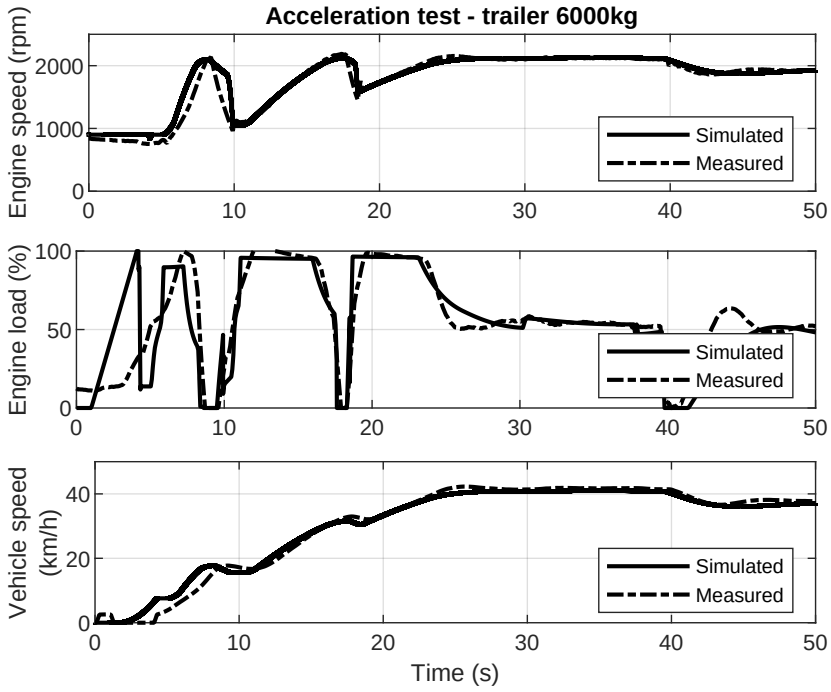

Figure 6. Performance comparison: model vs. experimental data.

Model performance was studied also looking at the engine behavior both in terms of rotational speed and actual engine load. As shown in Figure 6, a comparison between the simulated and measured engine speed was performed. This analysis was necessary to validate the speed controller model which during acceleration showed a close behavior to the real one given the same driver inputs of the experimental test. Another important comparison was made between the measured and simulated engine percentage load. The good results obtained allowed validating the engine model in terms of characteristic map which provided performance very close to the real engine under the same working conditions.

The validation of the powertrain parameters with a set of driving tests was important for the estimation of the PTO loads on those sessions where the use of an implement tool represented the main power consumption contribution. However, as for the case shown in Figure 7, it is very common that the tractor also needs to pull the implement during working operations. Thus, the engine load measured during those sessions was the result of both a load required to pull the implement and of a power transferred to the external device. The previous validation of the driveline performance allowed estimating the power consumption related to the tractor movements at a certain working speed. Thus, the PTO load applied by the external device was obtained by mean of a PI controller on an external torque actuator whose goal was to track the measured engine load during the simulation of a certain PTO task. With this simplified approach it was possible to obtain an estimation of the power demand during the experimental activities on each different PTO implement. The proposed approach allowed characterizing the PTO activities performed during the experimental session without any specific knowledge of the working principles of the devices. In Table 4, the main results of this characterization activity are summarized. The knowledge of the power characteristics in terms of average and peak power demand for those activities is crucial during the design of the electric system for a new hybrid electric tractor.

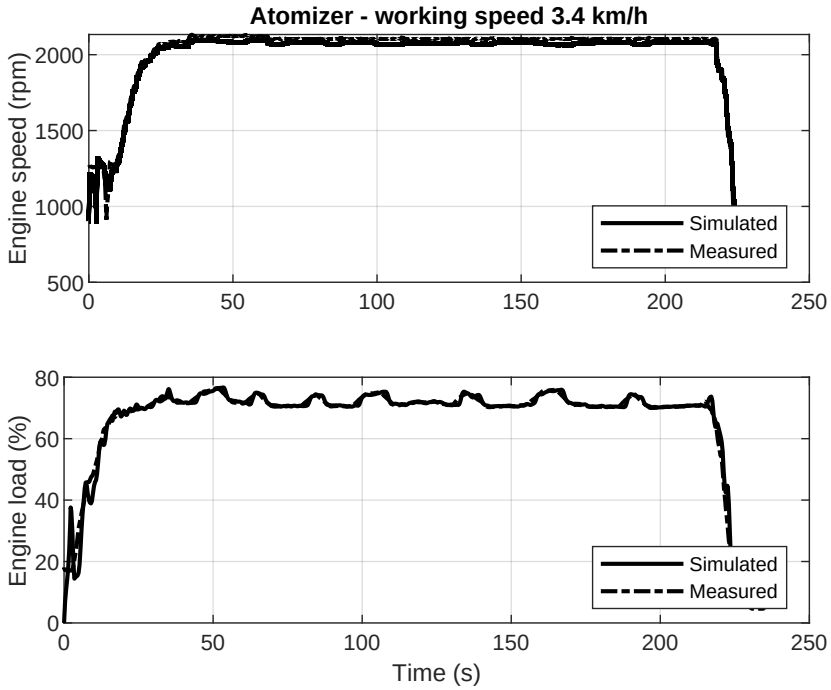

Figure 7. Performance comparison: model vs. experimental data.

Table 4. Statistics of the considered PTO working scenario—Power (kW).

	Atomizer	Shredder	Rotary Harrow
Min	34.5	12	35
Max	40	26	52
Mean	36	19	44
Std	1	2	3
Peak index	1.11	1.37	1.18

The results shown in Table 4 confirm that PTO loads were comparable, in terms of power demand, to the road transportation, confirming the multi-purpose nature of tractor machine. The most demanding activity measured and simulated surely was the harrowing. To be clear, harrowing also requires a high pulling force coming from the traction the tractor wheels are able to apply on the

terrain. Thus, this activity was actually involving both the driveline and the PTO with a comparable amount of power. Since the modeling of the terrain behavior during harrowing was not in the scope of this work, the same technique used to estimate the PTO loads in the case of an atomizer and a shredder was used to estimate the equivalent PTO load able to represent the harrowing action.

4.2. Performance Comparison: Hybrid vs. Diesel

In this section, performance of both the traditional diesel-powered model of the tractor and the proposed parallel hybrid electric architecture were compared. The comparison aimed to establish if the proposed hybrid architecture would be able to perform at least as well as the traditional one in terms of peak power capabilities estimating also the advantage in terms of energy consumption. The first comparison shown Figure 8 was performed on the acceleration test discussed in the previous section. This test was performed in both cases with the trailer at maximum load in order to be coherent with the experimental measurements. First, a good agreement in terms of engine speed can be highlighted. This result shows the stability of the Load Observer controller which managed the power split between the downsized diesel engine and the electric motor. A very stable behavior was achieved during gear shifts, which represent the most critical phase that could make the controller unstable due to the quick variation in terms of working condition. The Load Observer action can be highlighted when comparing the engine load during the same working task. The energy management strategy split the power output between the engine and the motor so that the overall output of the hybrid power unit was at the same level of the traditional architecture given the same task.

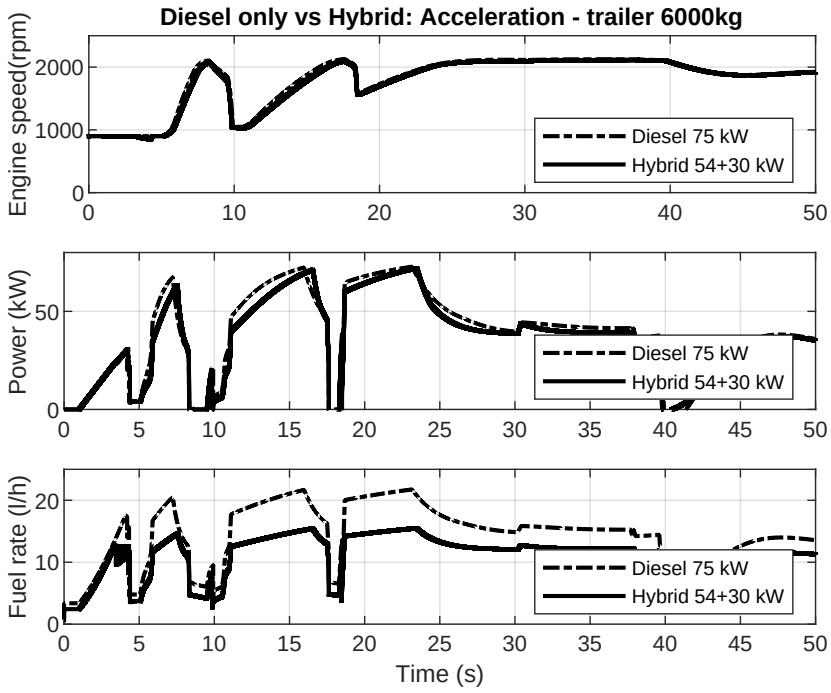

Figure 8. Hybrid vs. traditional architecture: acceleration test with full load trailer.

However, the most promising result is shown in the fuel rate estimation plot. In this work, the goal of the fuel consumption model was not to provide the exact value of the fuel usage but to have a tool to evaluate differences between the traditional and hybrid architecture. It is clear that the hybrid unit provided the same performance using less fuel than the diesel one for two main reasons. The smaller engine had an overall lower fuel consumption due to its size and to the fact that it is used closer to its nominal working condition (higher engine load). Thus, the engine also had better efficiency. Moreover, the use of the electric energy stored on the ESS reduced the amount of fuel required to accomplish a certain task. For the particular case of heavy road transportation, the overall reduction

of fuel usage can help in reducing the amount of harmful pollutants emitted by diesel engines on the roads. Moreover, the greener is the electric source from which the ESS of the vehicle is charged, the higher will be the positive impact of the lower fuel consumption on the tractor.

With the same approach, simulations were performed for the other working tasks derived from the experimental measurements on the tractor. In Figure 9, the simulation of the Rotary Harrow test is shown. This task was chosen due to the highly demanding power profile to test both the power capabilities of the hybrid power unit and its stability during heavy loads. During this activity the tractor moves at constant speed (usually around 3–5 km/h) pulling the rotary harrow on the terrain. Having said that, it is clear that the engine speed is practically constant during the task.

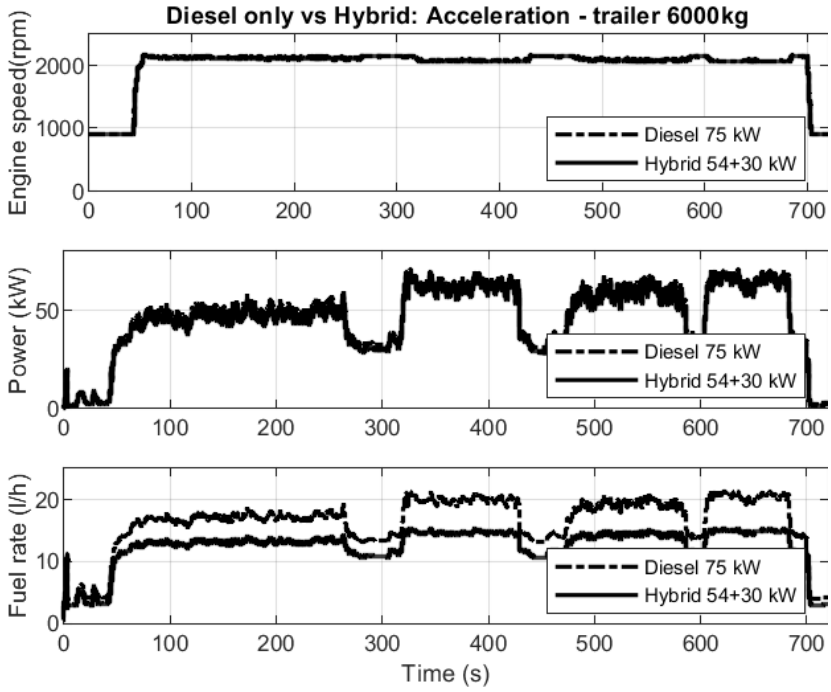

Figure 9. Hybrid vs. traditional architecture: rotary harrowing test.

However, results show a good engine speed stability regardless the high variability of the external load. In addition, in this case, the hybrid power unit was able to provide the same amount of power given by the traditional architecture using a downsized diesel engine with all the benefits already discussed. The lower fuel rate of the power unit obtained also in this simulation case confirms the benefits in terms of pollutant emission and cost savings. However, for operation on agriculture terrains such as the one simulated in this work, the lower fuel consumption reduces also the amount of pollutants that deposits on the soil, thus absorbed by the plant and eaten by the population. Table 5 summarizes the overall results obtained on all the activities simulated with both the models given the input signals derived from the measured data. In the table, an energy consumption comparison between the traditional power unit (ICE) and the hybrid one (ICE+EM) is performed. The estimated energy consumption both for the thermal engine and the electric motor were evaluated considering their average efficiency. In particular, for the engines, this value was obtained from energy content of the estimated fuel consumption scaled with an average of 20% efficiency for the diesel engine to make the fuel contribution comparable with the energy usage from the ESS. Given this comparison, it is possible to confirm what was previously discussed: the use of a smaller engine, optimized for the average load characteristic of the vehicle, helps also in improving the overall efficiency of the vehicle during all the proposed simulation scenarios. An average reduction of 16% in the energy consumption required to accomplish a task confirms that smaller diesel engines with the help of an electric system can perform better than bigger ones. Thus, it is possible to state that hybrid and electric

powertrains can effectively represent an alternative propulsion system for orchard tractors providing good performance in terms of peak power capabilities or same performance level but with a more efficient energy usage.

Table 5. Tasks experimental characterization overview: (a) Trailer 6000 kg; (b) Trailer 1400 kg; (c) Atomizer; (d) Shredder; and (e) Rotary harrow.

	a	**b**	**c**	**d**	**e**
Work time (h)	0.017	0.05	0.065	0.18	0.2
ICE (75 kW)	2.3	5.5	11.9	25.2	36
Hybrid	1.93	4.5	10	21.4	29.7
Energy (%)	−17%	−18%	−16%	−15%	−17%

5. Conclusions

In this work, a numerical model for a hybrid electric orchard tractor was designed to study performance of a parallel hybrid architecture according to realistic working scenarios. Tractors are multi-purpose machines and must be designed to meet the needs of the final users in terms of functionalities, flexibility, and power delivery. The lack of standardized testing cycles requires the analysis of real use cases to characterize the power demand of each task. In this work, an extensive preliminary data acquisition from a real working tractor was performed to have enough data to describe several working tasks. From the experimental data, a set of input signals for the two different models was derived. One model aimed to numerically replicate performance of the monitored diesel powered tractor, while the other was designed to study a parallel hybrid electric configuration. The traditional tractor model was validated comparing performance directly with the measured data. Moreover, the vehicle model proposed allowed estimating the PTO power demand during those operations when the engine was in charge of providing power both for the driveline-wheel subsystem and for the PTO implement. Thus, the working scenarios were applied to the proposed hybrid architecture. An energy management strategy called Load Observer was implemented in the simulated controller to properly split the power demand between the two propulsion units: a downsized diesel engine and an electric servomotor. Simulations showed not only that the proposed architecture was able to provide the same amount of power of the traditional tractor during different working conditions, but also that the use of a smaller engine is possible and allows using it more efficiently. The energy management strategy developed in this work was designed to prefer the thermal engine as primary energy source. This class of vehicles has very limited on-board space, thus also the size of the battery pack must be carefully optimized between performance improvements and vehicle integration needs. Moreover, the proposed energy management strategy aims to reduce the amount of batteries required for the battery pack. If costs are also taken into account, a poorly designed battery pack could lead to an increase of the overall cost of the vehicle in terms of TCO (Total Cost of Ownership), which could strongly affect the industrial success of the hybrid solution. Although the TCO of the hybrid solution can be lower if the difference in terms of fuel cost is considered (cost of diesel and of electricity), the initial cost difference should be reasonable to convince the final user to adopt the new technology. Since nowadays batteries represent one of the highest cost item of an electrified vehicle, the adoption of an energy management strategy which could effectively use at their best both the on-board energy reservoirs is mandatory and would translate into a reduction of the initial cost of the new hybrid technology. The benefits deriving from tractor electrification were highlighted by the simulation results. Their real environmental impact could be greater if, as often happens, the electricity stored on the ESS would come from green energy sources such as photovoltaic panels or wind turbines installed in or nearby the farm. The availability of green energy sources and of electrified agriculture machines will be the base element for the transition towards modern sustainable and smart farms.

Author Contributions: Conceptualization, F.M. and A.S.; methodology, F.M.; software, F.M.; formal analysis, F.M.; investigation, F.M. and A.S.; data curation, F.M. and A.S.; writing—original draft preparation, F.M.; writing—review and editing, F.M. and A.S.; visualization, F.M.; and supervision, A.S. All authors have read and agreed to the published version of the manuscript.

Funding: This research received no external funding.

Conflicts of Interest: The authors declare no conflict of interest.

References

1. Dons, E.; Laeremans, M.; Orjuela, J.P.; Avila-Palencia, I.; de Nazelle, A.; Nieuwenhuijsen, M.; Van Poppel, M.; Carrasco-Turigas, G.; Standaert, A.; De Boever, P.; et al. Transport most likely to cause air pollution peak exposures in everyday life: Evidence from over 2000 days of personal monitoring. *Atmos. Environ.* **2019**, *213*, 424–432. [CrossRef]
2. Catalano, M.; Galatioto, F. Enhanced transport-related air pollution prediction through a novel metamodel approach. *Transp. Res. Part D Transp. Environ.* **2017**, *55*, 262–276. [CrossRef]
3. Wei, H. Impacts of China's national vehicle fuel standards and subway development on air pollution. *J. Clean. Prod.* **2019**, *241*, 118399. [CrossRef]
4. Cepeda, M.; Schoufour, J.; Freak-Poli, R.; Koolhaas, C.M.; Dhana, K.; Bramer, W.M.; Franco, O.H. Levels of ambient air pollution according to mode of transport: A systematic review. *Lancet Public Health* **2017**, *2*, e23–e34. [CrossRef]
5. European Environment Agency. *Emissions of Air Pollutants from Transports*; European Environment Agency: Copenhagen, Denmark, 2019.
6. European Environment Agency. *Air Pollution Sources*; European Environment Agency: Copenhagen, Denmark, 2019.
7. European Parliament—Council of the European Union. *Directive 97/68/EC*; European Parliament—Council of the European Union: Bruxelles, Belgium, 1997.
8. European Parliament—Council of the European Union. *Directive 2004/26/EC*; European Parliament—Council of the European Union: Bruxelles, Belgium, 2004.
9. European Parliament—Council of the European Union. *Regulation (EU) 2013/167*; European Parliament—Council of the European Union: Bruxelles, Belgium, 2013.
10. European Parliament—Council of the European Union. *Regulation (EU) 2016/1628*; European Parliament—Council of the European Union: Bruxelles, Belgium, 2016.
11. Lovarelli, D.; Bacenetti, J. Exhaust gases emissions from agricultural tractors: State of the art and future perspectives for machinery operators. *Biosyst. Eng.* **2019**, *186*, 204–213. [CrossRef]
12. Grigoratos, T.; Fontaras, G.; Giechaskiel, B.; Zacharof, N. Real world emissions performance of heavy-duty Euro VI diesel vehicles. *Atmos. Environ.* **2019**, *201*, 348–359. [CrossRef]
13. Song, C.; Ma, C.; Zhang, Y.; Wang, T.; Wu, L.; Wang, P.; Liu, Y.; Li, Q.; Zhang, J.; Dai, Q.; et al. Heavy-duty diesel vehicles dominate vehicle emissions in a tunnel study in northern China. *Sci. Total Environ.* **2018**, *637–638*, 431–442. [CrossRef]
14. Jiang, Y.; Yang, J.; Cocker, D.; Karavalakis, G.; Johnson, K.C.; Durbin, T.D. Characterizing emission rates of regulated pollutants from model year 2012 + heavy-duty diesel vehicles equipped with DPF and SCR systems. *Sci. Total Environ.* **2018**, *619–620*, 765–771. [CrossRef]
15. Zheng, X.; Wu, Y.; Zhang, S.; Baldauf, R.W.; Zhang, K.M.; Hu, J.; Li, Z.; Fu, L.; Hao, J. Joint measurements of black carbon and particle mass for heavy-duty diesel vehicles using a portable emission measurement system. *Atmos. Environ.* **2016**, *141*, 435–442. [CrossRef]
16. Krishnamurthy, M.; Carder, D.K.; Thompson, G.; Gautam, M. Cost of lower NOx emissions: Increased CO2 emissions from heavy-duty diesel engines. *Atmos. Environ.* **2007**, *41*, 666–675. [CrossRef]
17. Xin, Q.; Xin, Q. Diesel aftertreatment integration and matching. *Diesel Engine Syst. Des.* **2013**, 503–525. [CrossRef]
18. Neeft, J.P.; Makkee, M.; Moulijn, J.A. Diesel particulate emission control. *Fuel Process. Technol.* **1996**, *47*, 1–69. [CrossRef]
19. Chou, C.H.; Chen, P.T.; Yang, C.J.; Huang, K.D. Functionalization of Wireless Control and Fuzzy Systems to Hybrid Mini-Loaders. *IEEE Access* **2020**, *8*, 80914–80921. [CrossRef]

20. Chen, P.T.; Ding, P.F.; Yang, C.J.; Huang, K.D. Hybrid Power System Design for Multifunctional Mini-Loader Vehicles. *Appl. Sci.* **2019**, *9*, 4439. [CrossRef]
21. Somà, A. *Trends and Hybridization Factor for Heavy-Duty Working Vehicles*; IntechOpen: Rijeka, Croatia, 2017; Chapter 1, doi:10.5772/intechopen.68296. [CrossRef]
22. Lajunen, A.; Sainio, P.; Laurila, L.; Pippuri-Mäkeläinen, J.; Tammi, K. Overview of Powertrain Electrification and Future Scenarios for Non-Road Mobile Machinery. *Energies* **2018**, *11*, 1184. [CrossRef]
23. Wang, J.; Yang, Z.; Liu, S.; Zhang, Q.; Han, Y. A comprehensive overview of hybrid construction machinery. *Adv. Mech. Eng.* **2016**, *8*, 1687814016636809. [CrossRef]
24. Somà, A.; Bruzzese, F.; Mocera, F.; Viglietti, E. Hybridization Factor and Performance of Hybrid Electric Telehandler Vehicle. *IEEE Trans. Ind. Appl.* **2016**, *52*, 5130–5138. [CrossRef]
25. Soma, A.; Mocera, F.; Bruzzese, F.; Viglietti, E. Simulation of dynamic performances of electric-hybrid heavy working vehicles. In Proceedings of the 2016 Eleventh International Conference on Ecological Vehicles and Renewable Energies (EVER), Monte Carlo, Monaco, 6–8 April 2016; pp. 1–8. [CrossRef]
26. Mocera, F.; Somà, A. Working Cycle requirements for an electrified architecture of a vertical feed mixer vehicle. *Procedia Struct. Integr.* **2018**, *12*, 213–223. [CrossRef]
27. Moreda, G.; Mu noz-García, M.; Barreiro, P. High voltage electrification of tractor and agricultural machinery—A review. *Energy Convers. Manag.* **2016**, *115*, 117–131. [CrossRef]
28. Florentsev, S.; Izosimov, D.; Makarov, L.; Baida, S.; Belousov, A. Complete traction electric equipment sets of electro-mechanical drive trains for tractors. In Proceedings of the 2010 IEEE Region 8 International Conference on Computational Technologies in Electrical and Electronics Engineering (SIBIRCON), Listvyanka, Russia, 11–15 July 2010; pp. 611–616. [CrossRef]
29. Troncon, D.; Alberti, L.; Mattetti, M. A Feasibility Study for Agriculture Tractors Electrification: Duty Cycles Simulation and Consumption Comparison. In Proceedings of the 2019 IEEE Transportation Electrification Conference and Expo (ITEC), Detroit, MI, USA, 19–21 June 2019; pp. 1–6. [CrossRef]
30. Lagnelöv, O.; Larsson, G.; Nilsson, D.; Larsolle, A.; Hansson, P.A. Performance comparison of charging systems for autonomous electric field tractors using dynamic simulation. *Biosyst. Eng.* **2020**, *194*, 121–137. [CrossRef]
31. Wu, Z.; Xie, B.; Li, Z.; Chi, R.; Ren, Z.; Du, Y.; Inoue, E.; Mitsuoka, M.; Okayasu, T.; Hirai, Y. Modelling and verification of driving torque management for electric tractor: Dual-mode driving intention interpretation with torque demand restriction. *Biosyst. Eng.* **2019**, *182*, 65–83. [CrossRef]
32. Melo, R.R.; Antunes, F.L.; Daher, S.; Vogt, H.H.; Albiero, D.; Tofoli, F.L. Conception of an electric propulsion system for a 9 kW electric tractor suitable for family farming. *IET Electr. Power Appl.* **2019**, *13*, 1993–2004. [CrossRef]
33. Kannusamy, M.Y.L.; Ravindran, V.; Rao, N. *Analysis of Multiple Hybrid Electric Concept in Agricultural Tractor through Simulation Technique*; SAE Technical Paper: Warrendale, PA, USA, 2019; doi:10.4271/2019-26-0243. [CrossRef]
34. Troncon, D.; Alberti, L.; Bolognani, S.; Bettella, F.; Gatto, A. Electrification of agricultural machinery: A feasibility evaluation. In Proceedings of the 2019 Fourteenth International Conference on Ecological Vehicles and Renewable Energies (EVER), Monte-Carlo, Monaco, 8–10 May 2019; pp. 1–7. [CrossRef]
35. Mocera, F.; Vergori, E.; Soma, A. Battery Performance Analysis for Working Vehicle Applications. *IEEE Trans. Ind. Appl.* **2020**, *56*, 644–653. [CrossRef]
36. Vergori, E.; Mocera, F.; Somà, A. Battery Modelling and Simulation Using a Programmable Testing Equipment. *Computers* **2018**, *7*, 20. [CrossRef]
37. Mocera, F.; Vergori, E.; Soma, A. Study of battery performance with hardware in the loop simulation of a working vehicle. In Proceedings of the 2018 13th International Conference on Ecological Vehicles and Renewable Energies, EVER, Monte-Carlo, Monaco, 10–12 April 2018; doi:10.1109/EVER.2018.8362399. [CrossRef]
38. Voss, W. *A Comprehensible Guide to Controller Area Network*; Copperhill Technologies Corporation: Greenfield, MA, USA, 2005.
39. Voss, W. *A Comprehensible Guide to J1939*; Copperhill Technologies Corporation: Greenfield, MA, USA. 2008.
40. Mathworks. *Getting Started with Simscape*; MathWorks: Natick, MA, USA, 2018.

41. Genta, G. *Motor Vehicle Dynamics: Modeling and Simulation*; World Scientific: Singapore, 1997.
42. Grasso, J.V.R.; Perumpral, D.; Vaughan, G.T.; Roberson, R.P. *Predicting Tractor Diesel Fuel Consumption*; Virginia Cooperative Extension: Blacksburg, VA, USA, 2010.